Contribution from the Service de Chimie Organique et de Chimie Organique Physique, Faculté des Sciences, Université Libre de Bruxelles, CP 160, 50 Avenue F. D. Roosevelt, B-1050 Bruxelles, Belgium

Ruthenium(II) Complexes of 1,4,5,8-Tetraazaphenanthrene (TAP) and 2,2′-Bipyridine (bpy). Ground- and Excited-State Basicities of $Ru^{2+}(bpy)_n(TAP)_{3-n}$ (n = 0, 1, 2): Their Luminescence Quenching by Organic Buffers

A. Kirsch-De Mesmaeker,* L. Jacquet, and J. Nasielski

Received February 10, 1988

1,4,5,8-Tetraazaphenanthrene (TAP) is a chelating ligand similar to 2,2′-bipyrazine (bpz), which differs from the latter by being much more rigid and having a more extended delocalized π-system. It was thus deemed interesting to compare the properties of three complexes, $Ru^{2+}(bpy)_n(TAP)_{3-n}$ (n = 0, 1, 2), with their corresponding $Ru^{2+}(bpy)_n(bpz)_{3-n}$ counterparts. The pK_a values of the singly protonated forms of the three TAP complexes in their ground and first excited MLCT states have been determined; the basicities increase with the increasing number of bpy ligands. In the pH range of the measurements, the protonation of the excited state is irreversible; the so-called "apparent pK_a^*'s" thus reflect only the sequence of the luminescence lifetimes, whereas the sequence of the basicities of the three complexes in their excited state follows that of the pK_a^*'s estimated from a Förster cycle. The complexes are more basic in the excited state than in the ground state. Interestingly, the luminescences are also quenched by organic buffers in pH domains where protonation cannot occur; this is attributed to the formation of hydrogen bonds between the carboxylic acid of the buffer with one of the free nitrogen atoms of the TAP ligand(s). It was also found that the quenching rate constant by the carboxylic acids decreases when the corresponding carboxylate ion is present; a mechanism is proposed where ion pairing is responsible for this loss of efficiency.

Introduction

A few years ago we studied the photoelectrochemistry of ruthenium(II) tris(tetraazaphenanthrene) ($Ru^{2+}(TAP)_3$) at a transparent SnO_2 electrode under continuous[1] and pulsed laser illumination.[2] The additional nitrogen atoms of TAP (I), as

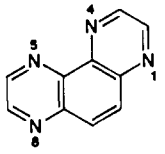

I

compared to those in bipyridine or phenanthroline, lead to complexes that are strongly oxidant in both the ground and MLCT excited states, as shown by the inability of $Ru^{2+}(TAP)_3^*$ to inject an electron in the conduction band of SnO_2. Only when hydroquinone is present, leading to a reductive quenching of the excited complex, is there a measurable photocurrent due to the oxidation of the photogenerated $Ru^+(TAP)_3$.[2]

The photoredox properties of $Ru^{2+}(TAP)_3$[3] are actually very similar to those of ruthenium(II) tris(2,2′-bipyrazine) ($Ru^{2+}(bpz)_3$) described and discussed previously by Lever and co-workers,[4,5] and both complexes share the structural property of having six free nitrogen atoms available for interactions with the surroundings. It has been shown, indeed, that the remote nitrogen atoms in complexes in the excited state and monoreduced form, with ligands such as bpz,[5,6] 2,2′-bipyrimidine,[7] and 2,2′-bibenzimidazole[8] give rise to protonations; thus, $Ru^{2+}(bpz)_3$ with its six free nitrogen atoms undergoes six distinct successive protonations in both its ground and excited states.[5]

With $Ru^{2+}(TAP)_3$, during the luminescence and photoelectrochemical experiments performed previously,[1-3] differences in luminescence intensities and photocurrents were observed in the presence and the absence of an acetic buffer in solution, suggesting a pH effect and interactions of the excited state with the buffer. Therefore, because of some similarities of TAP with bpz, TAP differing only from bpz by being much more rigid and having a more extended delocalized π-system, we engaged in a study of the ground- and excited-state basicity of the three complexes $Ru^{2+}(bpy)_n(TAP)_{3-n}$ (n = 0, 1, 2) and of their interaction with organic buffers; in this paper we present and discuss different mechanisms of interaction from data obtained under continuous and pulsed laser irradiation.

Experimental Section

$Ru^{2+}(TAP)_3$ was synthesized as described previously.[3] $Ru^{2+}(bpy)_2(TAP)$ was made by refluxing under argon a water–methanol (1/1 v/v) solution of 1 equiv of $Ru(bpy)_2Cl_2$[9] and 1 equiv of TAP.[10] $Ru^{2+}(bpy)(TAP)_2$ was obtained similarly by reacting under the same conditions 1 equiv of bpy with 1 equiv of $Ru(TAP)_2Cl_2$, which was made according to the method recommended for the synthesis of $Ru(bpy)_2Cl_2$.[9] The three complexes were purified by eluting them through a cation exchanger (Sephadex SP C25) with 0.1 M aqueous NaCl; the cations are precipitated by the addition of saturated aqueous KPF_6, filtered, and dried under reduced pressure. Their ^1H NMR spectra are in full agreement with the proposed structures and especially with their expected symmetry.[10]

The absorption spectra are recorded with a Varian-Cary 219 instrument. The emission intensities are measured perpendicularly to the excitation through an Applied Photophysics monochromator and with a Hamamatsu R 928 (for λ < 900 nm) or RCA 7102 (for λ > 900 nm) photomultiplier; the light source is a 250-W xenon arc lamp for continuous illumination or a Molectron UV 24 nitrogen laser (pulse width 8 ns) for lifetime measurements. The pulsed signal of the photomultiplier is fed to a Hewlett-Packard 54200 A digitizing oscilloscope, averaged over 16 pulses, corrected for the base line, and transferred to a Hewlett-Packard 9816 S microcomputer; the kinetic curves are fitted to the rate equation by a nonlinear least-squares regression program.[11]

Oleum (65% SO_3), sodium acetate, sodium citrate, citric acid, and sodium hydroxide were from Merck, and sulfuric acid was from UCB; all were high-purity analytical reagents and were used as supplied. Acetic

* To whom correspondence should be addressed. "Maître de Recherche", FNRS, Belgium.

(1) Kirsch-De Mesmaeker, A.; Maetens, D.; Nasielski-Hinkens, R. *J. Electroanal. Interfacial Electrochem.* **1985**, *182*, 123–132.
(2) Masschelein, A.; Kirsch-De Mesmaeker, A. *Nouv. J. Chim.* **1987**, *11*, 329–335.
(3) Kirsch-De Mesmaeker, A.; Nasielski-Hinkens, R.; Maetens, D.; Pauwels, D.; Nasielski, J. *Inorg. Chem.* **1984**, *23*, 377–379.
(4) (a) Crutchley, R. J.; Lever, A. B. P. *J. Am. Chem. Soc.* **1980**, *102*, 7128–7129. (b) Crutchley, R. J.; Lever, A. B. P. *Inorg. Chem.* **1982**, *21*, 2276–2282. (c) Gonzales-Velasco, J.; Crutchley, R. J.; Lever, A. B. P.; Bard, A. J. *Inorg. Chem.* **1983**, *22*, 822–825.
(5) (a) Crutchley, R. J.; Kress, N.; Lever, A. B. P. *J. Am. Chem. Soc.* **1983**, *105*, 1170–1178. (b) Haga, M. A.; Dodsworth, E. S.; Eryavec, G.; Seymour, P.; Lever, A. B. P. *Inorg. Chem.* **1985**, *24*, 1901–1906.
(6) Venturi, M.; Mulazzani, Q. G.; Ciano, M.; Hoffman, M. Z. *Inorg. Chem.* **1986**, *25*, 4493–4498.
(7) (a) Maetens, D.; Nasielski, J.; Nasielski-Hinkens, R. *J. Organomet. Chem.* **1979**, *168*, 177. (b) Rillema, D. P.; Allen, G.; Meyer, T. J.; Conrad, D. *Inorg. Chem.* **1983**, *22*, 1617–1622.
(8) Bond, A. M.; Haga, M. A. *Inorg. Chem.* **1986**, *25*, 4507–4514.
(9) Sullivan, B. P.; Salmon, D. J.; Meyer, T. J. *Inorg. Chem.* **1987**, *17*, 3334.
(10) Masschelein, A., paper to be submitted for publication.
(11) (a) Wentworth, W. E. *J. Chem. Educ.* **1965**, *42*, 96–103. (b) Wentworth, W. E. *J. Chem. Educ.* **1965**, *42*, 162–167. (c) Demas, J. N. *Excited State Lifetime Measurements*; Academic: New York, 1983.

0020-1669/88/1327-4451$01.50/0

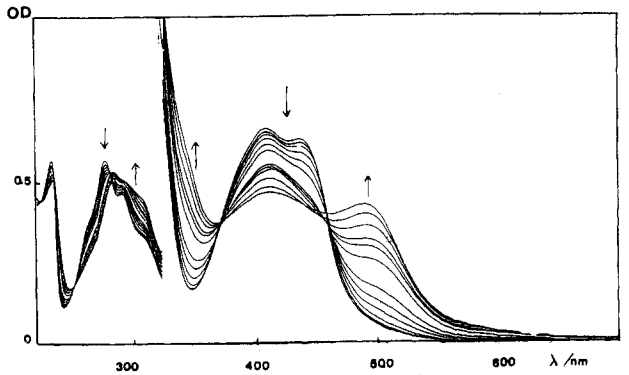

Figure 1. Absorption spectra of 5×10^{-5} M $Ru^{2+}(TAP)_3$ for increasing protonating powers of the solution: H_0 = −0.20, −0.72, −1.33, −1.72, −2.04, −2.26, −2.73, −3.06, −3.30, −3.58, −3.77, −4.09. The correspondence between the H_0 values and the different percentages of added sulfuric acid are from ref 20.

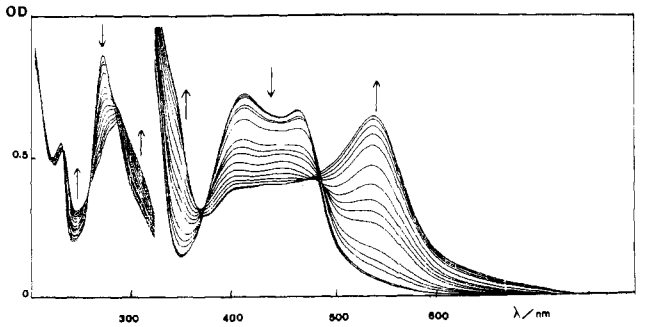

Figure 2. Absorption spectra of 5×10^{-5} M $Ru^{2+}(TAP)_2(bpy)$ for increasing protonating powers of the solution: H_0 = 0.1, −0.65, −1.40, −1.57, −1.83, −2.26, −2.44, −2.59, −2.85, −3.15, −3.49, −3.77, −4.0, −4.24, −4.34.

acid was distilled over $KMnO_4$, and water was purified with a Milli-Q water purification system. Aqueous ammonium persulfate was precipitated with ethanol to remove unwanted ammonium sulfate.

Results and Discussion

1. Protonations of the Ground State. Figure 1 shows the evolution of the absorption spectra of $Ru^{2+}(TAP)_3$ with the protonating power of the medium. From H_0 = 0 to −4, the MLCT band (λ_{max} = 407 and 436 nm) decreases; a new band appears near 500 nm and gradually shifts to 495 nm at higher acidities. A further increase of acidity from H_0 = −4 to −5 (not shown) leads to a still more marked drop of the 407–436-nm band, while the long-wavelength absorption increases and shifts from 495 to 485 nm; these trends continue steadily between H_0 = −5 and −11. The final situation is reached in oleum (65% SO_3), where the MLCT band looks about the same as that observed in neutral solution (Figure 4A) except for a moderate red shift of about 20 nm (430 and 452 nm). All these changes are fully reversible as shown by a complete return to the original spectrum after neutralization.

This behavior is quite similar to that described for $Ru^{2+}(bpz)_3$[5] but not identical since in the case of $Ru^{2+}(TAP)_3$ there is no well-defined H_0 range where there are clear-cut isobestic points; instead, we observe a constant shift of the crossings and it is not possible to identify the six successive protonations corresponding to the six available nitrogen atoms.

The first protonation induces a strong red shift of the MLCT band because of the stabilization of the π^* orbital. We postpone the discussion about the hexaprotonated complex until the end of this section.

Figure 2 shows the evolution of the absorption of the second complex $Ru^{2+}(bpy)(TAP)_2$ as a function of acidity. From H_0 = 0 to −4.3, the MLCT band (λ_{max} = 412 and 465 nm) decreases while a new band appears at 540 nm. From H_0 = −4.3 to −6.5 (not shown), the absorptions around 440 nm continue to decrease while the 540-nm band increases, broadens, and shifts to the blue (534 nm). From H_0 = −6.5 to −9.4, a new maximum appears at 430 nm, while the long-wavelength band shifts now from 534 to 542 nm and shows a further increase. The spectrum in oleum (Figure 4B) is quite different from the one in neutral solution.

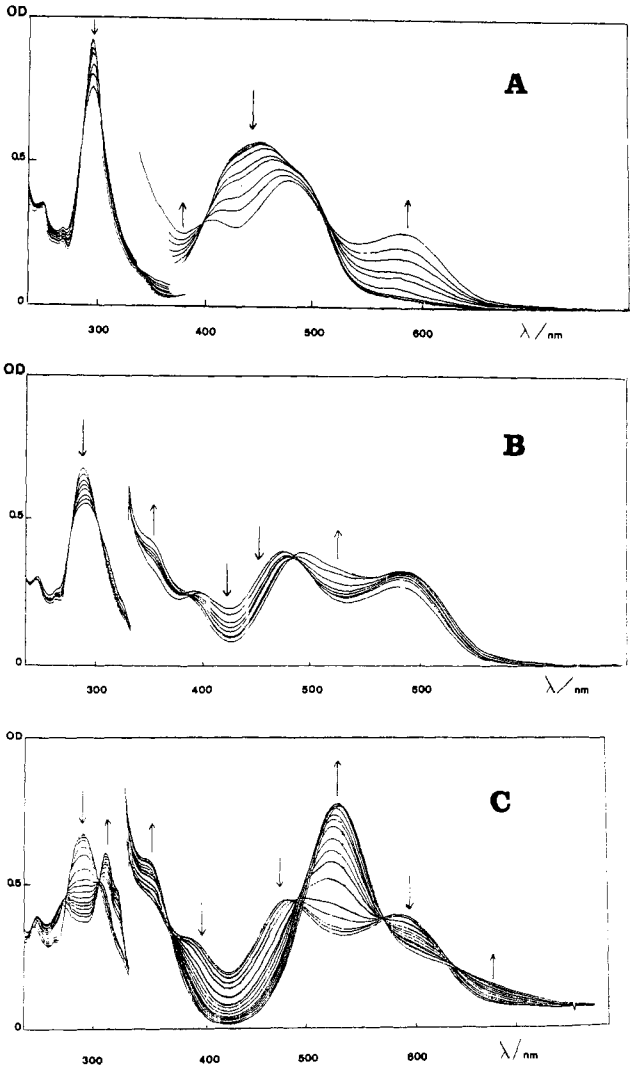

Figure 3. Absorption spectra of 5×10^{-5} M $Ru^{2+}(TAP)(bpy)_2$ for increasing protonating powers of the solution: (A) H_0 = −0.28, −0.41, −0.91, −1.28, −1.42, −1.66, −1.83, −2.06, −2.26; (B) H_0 = −2.26, −2.44, −2.58, −2.72, −2.90, −3.12, −3.34, −3.40; (C) H_0 = −2.90, −3.08, −3.23, −3.51, −3.78, −4.20, −4.50, −4.70, −4.93, −5.26, −5.54, −5.77, −6.15, −6.65, −7.33, −8.42.

The changes of the absorption spectrum of the third complex $Ru^{2+}(bpy)_2(TAP)$ with increasing acidity are shown in Figure 3. Here again, the MLCT band (λ_{max} = 445 nm) loses intensity between H_0 = 0 and −2.26 (Figure 3A) while a new band appears at 580 nm. When the acidity is increased from H_0 = −2.26 to −3.4 (Figure 3B), the original MLCT band continues to decrease, and some absorption gradually appears between 500 and 550 nm, which eventually results in a new maximum at 530 nm at H_0 = −8.4 (Figure 3C), accompanied by the disappearance of the absorption at 580 nm. The spectrum in oleum (Figure 4C) is very different from that observed in the neutral medium.

A comparison of parts A–C of Figure 4 discloses an intriguing behavior of the three complexes. Whereas $Ru^{2+}(TAP)_3$ and its fully protonated (six protons) form have similar absorption spectra, this does not hold for the two mixed complexes: the fully protonated forms of $Ru^{2+}(bpy)(TAP)_2$ (four protons) and $Ru^{2+}(bpy)_2(TAP)$ (two protons) show spectra that are vastly different from those of their unprotonated counterparts. This observation is quite unexpected and warrants some discussion. The first example of a complex showing a strong similarity between the spectra in neutral medium and in strong acid was given by Lever and co-workers[5] for their $Ru^{2+}(bpz)_3$; their interpretation is that partially protonated forms lose the original D_3 symmetry, with the consequence that formerly forbidden transitions become al-

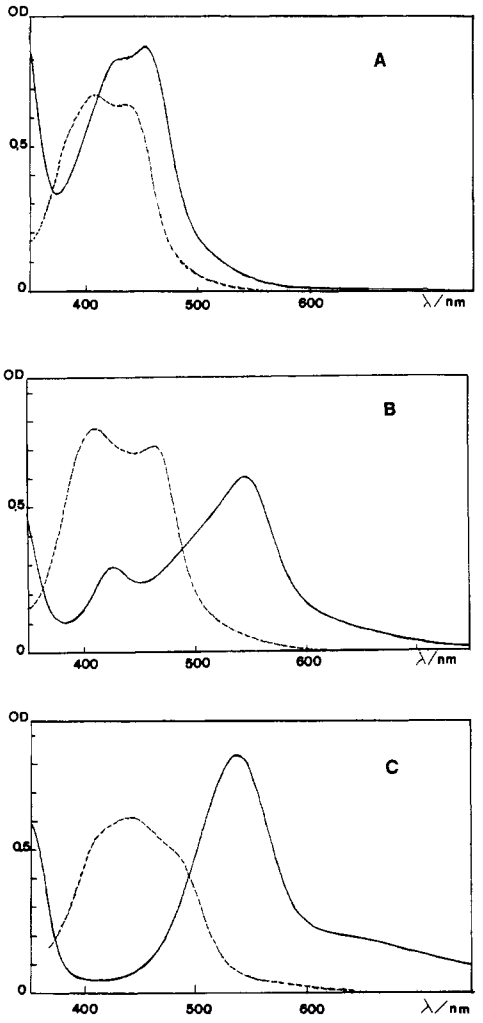

Figure 4. Comparison of the absorption spectra of the three complexes (5×10^{-5} M) in neutral solution (---) and in 60% oleum (—): (A) $Ru^{2+}(TAP)_3$; (B) $Ru^{2+}(TAP)_2(bpy)$; (C) $Ru^{2+}(TAP)(bpy)_2$.

lowed, but that full protonation restores the D_3 symmetry and a spectrum is obtained which is similar to the starting one. Our results with $Ru^{2+}(TAP)_3$, which has D_3 symmetry in neutral solution and in oleum, confirm these results and seem to strengthen the interpretation. Turning now to $Ru^{2+}(bpy)(TAP)_2$, we see that the starting ion and its fully protonated form have C_2 symmetry, whereas most of the intermediates lose it. Should symmetry arguments be applicable to this case, one would expect a strong similarity between the spectra of $Ru^{2+}(bpy)(TAP)_2$ and $Ru(bpy)(TAP)_2H_4^{6+}$, and this is contradicted by the data; the same reasoning applied to $Ru^{2+}(bpy)_2(TAP)$ gives the same prediction and leads to the same contradiction with the facts. It is thus clear that symmetry considerations alone are not sufficient to explain the data.

We want to suggest that another factor should be considered: the value of an oriented intramolecular electric field. In the four species $Ru^{2+}(bpz)_3$, $Ru(bpz)_3H_6^{8+}$, $Ru^{2+}(TAP)_3$, and $Ru(TAP)_3H_6^{8+}$, the metal ion is in an electric field having D_3 symmetry devoid of any dipolar component. The mixed complexes, in their unprotonated forms $Ru^{2+}(bpy)(TAP)_2$ and $Ru^{2+}(bpy)_2(TAP)$, have C_2 symmetry and the metal ion is in an electric field whose vector coincides with this C_2 axis, and thus has a dipolar component, whose value is strongly increased upon protonation. The metal ion in the fully protonated cations is thus in a very strong linear electric field that can profoundly alter the energy of the relevant electronic levels. We feel that such oriented electric fields certainly play a major part in our observations and have to be considered in addition to the symmetry arguments.

2. pK_a of the Ground States. A reliable spectrophotometric determination of pK_a's requires well-defined isosbestic points

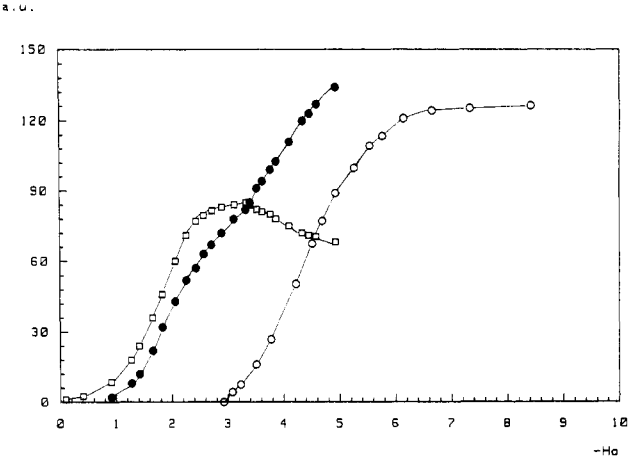

Figure 5. Absorption (in arbitrary units) plotted versus H_0 for $Ru^{2+}(bpy)_2(TAP)$: (●) 280 nm; (○) 530 nm; (□) 580 nm.

extending in an appreciable range of proton activity or pH values of the medium. For successive protonations of a structure having more than one basic site, this amounts to having two successive forms separated by at least 3 and preferably 4 pK_a units in order to have only one acid–base couple in a sufficiently broad H_0 domain. It is clear that this cannot be the case for $Ru^{2+}(TAP)_3$, where six successive pK_a's have to be squeezed between $H_0 = 0$ and −11.0, nor for $Ru^{2+}(bpy)(TAP)_2$, where the range $H_0 = 0$ to −9.4 has to accommodate four equilibria. One might hope to find a good case with $Ru^{2+}(bpy)_2(TAP)$, where two protonations occur in the range $H_0 = 0$ to −8.4, but even there this was not the case. We are thus dealing with three complexes showing more than two species in most H_0 domains. This can be demonstrated by using the method ingeniously applied to the anologous bpz complexes by Lever and co-workers:[5] if two species both absorb at wavelengths λ_1 and λ_2, and their equilibrium ratio is a function of H_0, the absorbance variations ΔA_{λ_1} and ΔA_{λ_2} are linearly related to each other for a range of H_0 values, and the corresponding straight line extrapolates to zero. The application of this procedure to the series $Ru^{2+}(bpy)_n(bpz)_{3-n}$ ($n = 0, 1, 2$) was successful and led to a reliable pK_a estimate for four out of the six successive protonations of $Ru^{2+}(bpz)_3$.[5] When applied to the present complexes, this method gives straight lines but the range of H_0 values where straight lines are found is so narrow that we cannot trust the results; it is clear, indeed, that, given a sufficiently narrow H_0 domain, a reasonable straight line will always result from such a treatment but whose significance is of course highly questionable.

Our failure to reliably identify the successive protonations may stem from the fact that the pK_a values are too close to each other, from solvatochromic shifts due to the varying polarity of the medium in addition to halochromic shifts or from a different sensitivity of the pK_a's of isomeric conjugate acids to solvent polarity. Whatever the real reason might be, there remains a sharp difference in behavior between $Ru^{2+}(bpz)_3$ and $Ru^{2+}(TAP)_3$, and we have not been able to think of an acceptable origin for this difference.

Because of these problems, only the pK_a values for the first protonations have been estimated, except for $Ru^{2+}(bpy)_2(TAP)$, where the second protonation could be examined. Two methods have been used.

In the first method, we plot the absorption at a given wavelength against H_0 in order to obtain a titration curve. The best choice of wavelength is of course that showing the largest difference of ϵ between the two species considered. Figure 5 shows such titration curves for $Ru^{2+}(bpy)_2(TAP)$ at 280 nm (both forms absorb), 580 nm (mainly monoprotonated), and 530 nm (mainly diprotonated).

The second method applies the equation

$$[B_i]/[B] = 1 + a_{H^+}/K_a = (A_i - A_f)/(A - A_f) \quad (1)$$

where $[B_i]$ stands for the initial concentration of the conjugate base, [B] stands for its actual concentration for a given proton activity a_{H^+} (corresponding to the H_0 value used), A_i and A denote

Table I. pK_a Values of the Complexes Determined at Different Wavelengths, from the Titration Curve (a) and from Eq 1 (b)[a]

complex	λ, nm	pK_{a_1}(a)	pK_{a_1}(b)	cc	pK_{a_2}(a)	pK_{a_2}(b)	cc
$Ru^{2+}(TAP)_3$	350	−3.0	−2.8	0.9855			
	410	−3.0	−3.0	0.9976			
$Ru^{2+}(TAP)_2(bpy)$	274	−2.6	−2.6	0.9959			
	510	−2.6	−2.4	0.9941			
	540	−2.6	−2.5	0.9934			
$Ru^{2+}(TAP)(bpy)_2$	280	−2.0	−1.9	0.9910	−4.6	−4.6	0.9964
	440	−2.0	−1.8	0.9956			
	530				−4.5		
	580	−2.0					

[a] cc = correlation coefficient for the straight line corresponding to eq 1.

Table II. Luminescence λ_{max} (Corrected for the Photomultiplier Response) and Lifetimes of the Basic Form (B), of the Monoprotonated Form (A), and of the Totally Protonated Form (A') for the Three Complexes[a]

complex	λ_{max}^{em}(B), nm	τ(B), ns	λ_{max}^{em}(A), nm	τ(A), ns	λ_{max}^{em}(A'), nm
$Ru^{2+}(TAP)_3$	595	230	800	<30	610
$Ru^{2+}(TAP)_2(bpy)$	640	620	900	<10	
$Ru^{2+}(TAP)(bpy)_2$	720	130	≥1020	<10	

[a] The lifetimes are given in the presence of air.

the corresponding absorbances, and A_f stands for the absorbance reached when all of the base form has been used up. K_a is then found from the straight line obtained by plotting $(A_i - A_f)/(A - A_f)$ vs a_{H^+}. Despite some ambiguity in the right choice of the A_f and A_i values, this method seems to work reasonably well; Table I gives the pK_a values for the three complexes, determined at various wavelengths by both methods. In spite of the difficulties encountered with our systems, the agreement between the results found by both methods is gratifying.

The pK_a's of Table I are the phenomenological values and not those pertaining to a specific protonation site; a detailed discussion of structure–property relations should thus include the statistical factor of 6 in the case of $Ru^{2+}(TAP)_3$, of 4 for $Ru^{2+}(bpy)(TAP)_2$, and of 2 for $Ru^{2+}(bpy)_2(TAP)$. When this correction is applied, the three pK_a's, which were −3.0, −2.6, and −2.0, respectively, become −3.8 for one of the six free nitrogen atoms of $Ru^{2+}(TAP)_3$, −3.2 for one of the four free nitrogen lone pairs of $Ru^{2+}(bpy)(TAP)_2$, and −2.3 per available site of $Ru^{2+}(bpy)_2(TAP)$.

As expected, the basicity of the first free nitrogen atom of the TAP ligands increases with the increasing number of bpy ligands. This is due to the stronger σ-donor property of bpy as compared with that of TAP, as illustrated by the first basicity of the two ligands (bpy, $pK_{a_1} = 4.45$;[12] TAP, $pK_{a_1} = 1.8$[13]), and to the stronger back-bonding effect[7a] of the TAP π* orbital, as explained also for the bpz and 2,2′-bipyrimidine ligands.[7b]

It has been possible to determine an approximate pK_a value for the second protonation of $Ru^{2+}(bpy)_2(TAP)$. Rather unexpectedly, it is only 2.6 pK_a units below pK_{a_1}; this explains why, even in this case, more than two species are detectably present throughout the useful H_0 range.

3. Luminescence as a Function of pH. The luminescence of $Ru^{2+}(TAP)_3$ at 595 nm (Table II; Figure 6) decreases as the pH is brought from 5 to 2, while a new, short-lived (less than 30 ns; Table II), and weaker emission grows around 800 nm. This luminescence remains unaltered between pH = 2 and $H_0 = -0.5$ and is to be assigned to the monoprotonated excited state of the complex. At still higher acidities, the 800-nm emission fades, and no other emission is detected until $H_0 = -11$, when a new luminescence is observed around 610 nm (Figure 6) having a lifetime of approximately 35 ns; this weak emission would correspond to the hexaprotonated complex and appears in the same spectral region as that of the nonprotonated excited species.

The two mixed complexes behave similarly on decreasing the pH: while the luminescence of the basic form decreases, there is a growing in of a weak, strongly red-shifted emission of the monoprotonated species, showing a lifetime shorter than 10 ns. No emission was detected from the other protonated species.

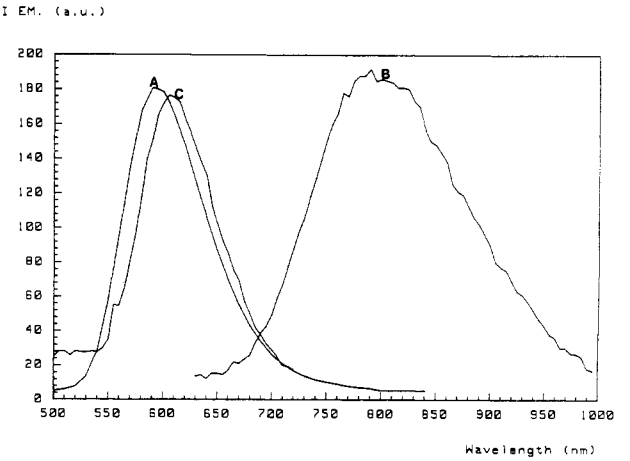

Figure 6. Emission spectra of $Ru^{2+}(TAP)_3$ at different pH values, recorded with different sensitivities of the photomultiplier: (A) in neutral solution; (B) from pH 2 to $H_0 = -0.5$; (C) in 60% oleum.

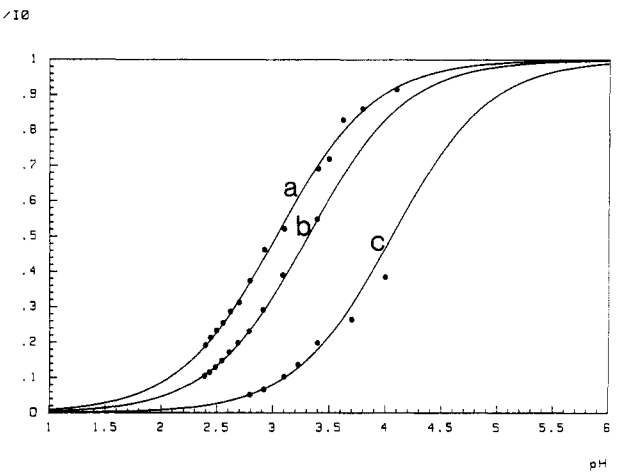

Figure 7. Luminescence intensity versus pH (non-degassed solutions): (a) $Ru^{2+}(TAP)(bpy)_2$; (b) $Ru^{2+}(TAP)_3$; (c) $Ru^{2+}(TAP)_2(bpy)$. No experimental points are obtained for (c) at pH ≥ 4.5 because those pH values cannot be obtained without buffer; curve c at those pH values has been calculated from the extrapolation of the straight line obtained by plotting I_0/I versus $[H^+]$.

Table III[a]

complex	pK_{a_1}*(app)	pK_{a_1}*(F)	$10^{-3}k_1\tau_0$, M^{-1}	log $(k_1\tau_0)$
$Ru^{2+}(TAP)_3$	3.5	5.0	2.3	3.36
$Ru^{2+}(TAP)_2(bpy)$	4	6.0	6.2	3.79
$Ru^{2+}(TAP)(bpy)_2$	3.1	≥6.4	1.3	3.11

[a] Definitions: $pK_{a_1}(app)^*$ = apparent $pK_{a_1}^*$; $pK_{a_1}(F)$ = Förster's $pK_{a_1}^*$; k_1 = protonation quenching rate constant. $k_1 = 1 \times 10^{10}$ M^{-1} s^{-1}.

(12) Nakamoto, K. *J. Phys. Chem.* **1960**, *64*, 1420–1425.
(13) Nasielski-Hinkens, R., private communication.

4. Determination of the First Protonation pK_a in the Excited State (pK_{a_1}*). Apparent pK_{a_1}. The inflection point in a luminescence intensity versus pH (or H_0) plot gives a pK_a (Figure 7) that is called "apparent" because it is not known a priori whether it corresponds to a true thermodynamic acid–base equilibrium in the excited state. The apparent pK_{a_1}* values of the three complexes are given in Table III. It is seen that the excited states are stronger bases than the ground states; the values, however, indicate no trend in the basicity as a function of the number of bpy ligands attached to the metal. The enhanced proton affinity of TAP in the excited state is of course to be related to the fact that the excitation entails a metal-to-ligand charge transfer (MLCT), increasing thus the electron density in the π^* orbital of the diimine ligands. This observation is consistent with the findings of Lever and co-workers[5] on the corresponding bpz complex.

Förster pK_{a_1}*. pK_{a_1}* can also be deduced[14,15] on the basis of a Förster cycle from the data in Table II, by use of eq 2, where ν_A and ν_B are the wavenumbers of the 0–0 transition in the emission spectrum of the acid and base forms, respectively, and the entropy

$$pK_a^* = pK_a + (0.625/T)(\nu_B - \nu_A) \quad (2)$$

changes accompanying protonation are assumed to be the same in the ground and excited states. The Förster pK_{a_1}* values of the three complexes deduced from eq 2 are given in Table III.

It must however be noticed that we have used the emission maxima for ν_B and ν_A and not the 0–0 transitions. A better evaluation of the 0–0 energy might come from a detailed analysis of the vibrational structure in the emission at low temperature, as was done by Meyer and co-workers.[16] If we remember, however, that the emission bands of our complexes have similar widths (the width at half height is 2450 ± 50 cm^{-1} for the basic form of the complexes), we feel safe in assuming that the energy differences between the Francke–Condon and 0–0 transitions will be fairly constant for all spectra and thus should lead to a fairly reliable pK_a sequence.

A second source of error lies in the fact that the monoprotonated mixed complexes emit in the near-infrared end of the spectrum (880 and 1000 nm), where the corrections for the phototube response are rather important, and at 1000 nm they are unreliable. After correction, the emission maximum recorded at 880 nm shifts to 900 nm and that found at 1000 nm must shift at least to 1020 nm and probably to a still longer wavelength.

The Förster pK_a* values for the three complexes are collected in Table III; they have been calculated from ground-state basicities uncorrected for the statistical factor and are, here again, overall phenomenological values. We shall restrict our discussion to these values because of the questionable use of a statistical factor in the MLCT state of $Ru^{2+}(TAP)_3$, which, similarly to $Ru^{2+}(bpy)_3$, has probably lost its ground-state D_3 symmetry[17] owing to the well-known charge localization on a single ligand out of the three accompanying the Jahn–Teller distortion of the excited state.

The Förster pK_a* values of Table III confirm the trend found in the ground state; i.e., the excited complexes are more basic when they contain more bpy ligands, which, being better σ-donors than TAP, increase the basicity of the $(Ru^{3+}–TAP^{\bullet-})$* fragment.

The ligand effect on basicity can also be correlated with that on the absorption and emission λ_{max} of the complexes (Table II), showing a red shift from $Ru^{2+}(TAP)_3$ to $Ru^{2+}(TAP)(bpy)_2$. This shift has also been observed and discussed by Meyer et al.[7] for the mixed-ligand complexes of bpy, bpz, and bpym, in terms of increasing stabilization of the excited chromophores $[Ru^{3+}–bpz^-]$* and $[Ru^{3+}–bipym^-]$* with the number of bpy ligands.

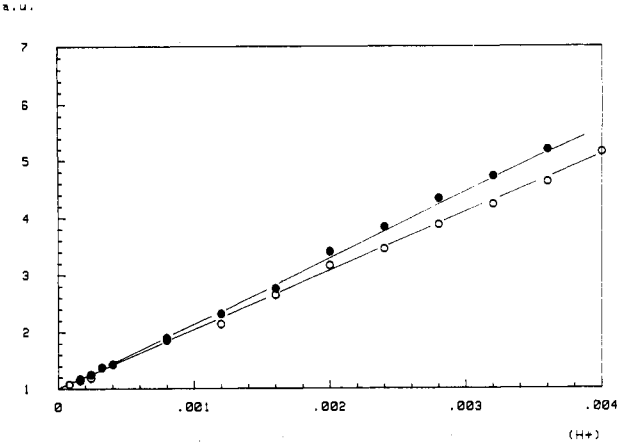

Figure 8. I_0/I (○) and τ_0/τ (●) versus $[H^+]$ for $Ru^{2+}(bpy)(TAP)_2$ (non-degassed solutions). The presence of air does not affect the quenching rate constant.

Scheme I

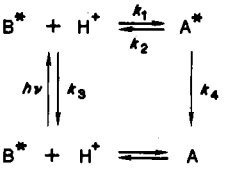

Quenching Rate Constants. Another approach for the determination of pK_a* is to examine the kinetics of the luminescence decay as a function of acidity. The emissions of the basic forms of the TAP complexes decay according to a strictly monomolecular process in the whole pH domain where the lifetimes are measurable ($\tau > 20$ ns). This indicates that the decay of B* is not perturbed by the deprotonation of A*, if the acid–base equilibrium is not reached during the excited-state lifetime. (See Scheme I.)

Moreover, plots of τ_0/τ and I_0/I for the basic form (where τ_0 and I_0 are the lifetimes and luminescence intensities of B* at a pH where quenching is absent) versus the concentration of H^+ give straight lines, with the same slope within experimental error (Figure 8). This suggests, as also concluded from the single-exponential luminescence decays, that the protonation of B* may be considered as irreversible. The equations for I_0/I and τ_0/τ may then be calculated as follows.

From Scheme I, one obtains under steady-state illumination

$$I_0/I = 1 + (k_1\tau_0[H^+])/(1 + k_2\tau_0') \quad (3)$$

where $\tau_0' = 1/k_4$ corresponds to the lifetime of A* at an H_0 value where the acid–base equilibrium is completely shifted toward A*. If the protonation of B* is irreversible, $k_2\tau_0'$ becomes negligible versus 1, and eq 3 simplifies to

$$I_0/I = 1 + k_1\tau_0[H^+] \quad (4)$$

Moreover, under that condition of irreversibility, τ_0/τ becomes equal to I_0/I (eq 4), in agreement with the obtained results (see Figure 8). Table III gives the values of $k_1\tau_0$ and k_1 determined from the slopes of these Stern–Volmer plots; for the three complexes $k_1 \approx 1 \times 10^{10}$ M^{-1} s^{-1} and the excited-state protonation is thus diffusion-controlled. On the other hand, since $k_2\tau_0'$ is small versus 1, k_2 cannot be obtained and the kinetic approach does not allow the determination of pK_{a_1}*.

5. Apparent vs Förster pK_{a_1}* Values. One can verify a posteriori that we are indeed dealing with systems where excited-state protonations are irreversible. The pK_{a_1}* values calculated from Förster's cycles being on the order of 6, with the protonation rate constant $k_1 = 1 \times 10^{10}$ M^{-1} s^{-1}, the deprotonation rate constant,

(14) Forster, T. *Naturwissenschaften* **1949**, *36*, 186.
(15) Weller, A. *Prog. React. Kinet.* **1961**, *1*, 189–214.
(16) (a) Allen, G. H.; White, R. P.; Rillema, D. P.; Meyer, T. J. *J. Am. Chem. Soc.* **1984**, *106*, 2613–2620. (b) Caspar, J. V.; Meyer, T. J. *J. Am. Chem. Soc.* **1983**, *105*, 5583–5590. (c) Kober, E. M.; Caspar, J. V.; Lumpkin, R. S.; Meyer, T. J. *J. Phys. Chem.* **1986**, *90*, 3722–3734. (d) Rillema, D. P.; Taghdiri, D. G.; Jones, D. S.; Keller, C. D.; Worl, L. A.; Meyer, T. J.; Levy, H. A. *Inorg. Chem.* **1987**, *26*, 578–585.
(17) According to ESR data, the electron hops among ligands in reduced Ru complexes on a nanosecond time scale: (a) Ohsawa, Y.; Hanck, K. W.; De Armond, M. K. *J. Electroanal. Chem. Interfacial Electrochem.* **1984**, *175*, 229–240. (b) Gex, J. N.; De Armond, M. K.; Hanck, K. W. *J. Phys. Chem.* **1987**, *91*, 251–254.

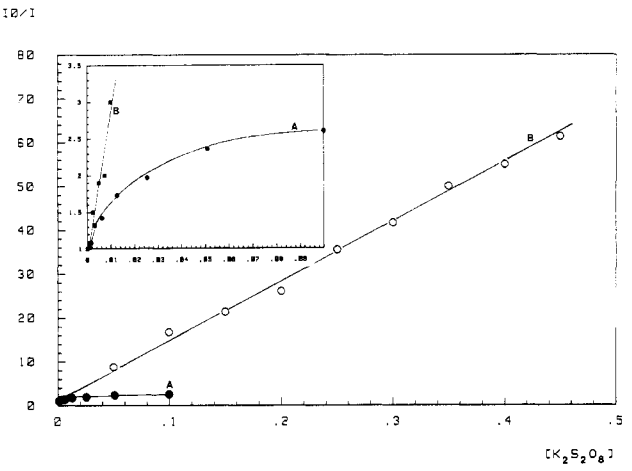

Figure 9. I_0/I or τ_0/τ for 5×10^{-5} M $Ru^{2+}(TAP)_3$ versus the $S_2O_8^{2-}$ concentration: (A) in the presence of the 0.5 M acetic acid–acetate buffer; (B) without buffer.

k_2, should be on the order of 10^4 s^{-1}. Thus, for a lifetime of the protonated form of 10 ns, $k_2\tau_0' = 10^4 \times 10^{-9} = 1 \times 10^{-4}$, which is indeed negligible versus 1.

Conversely, one can estimate the order of magnitude of $pK_{a_1}^*$ from a rough evaluation of the rate constants: $k_2\tau_0'$ will be considered negligible versus 1, as soon as k_2 is less than 10^6 s^{-1}; thus with $k_1 = 10^{10}$ M^{-1} s^{-1}, the real $pK_{a_1}^*$ should be greater than or equal to $-\log (10^6/10^{10}) = 4$, which is indeed the case of $pK_{a_1}^*$ calculated from the Förster cycle.

Considering now the apparent $pK_{a_1}^*$'s, it can be inferred from eq 3 that the inflection of the I/I_0 vs pH curve occurs at pH = $[\log (k_1\tau_0)]/(1 + k_2\tau_0')$; since $k_2\tau_0' \ll 1$, the apparent $pK_{a_1}^*$ becomes equal to $\log (k_1\tau_0)$. As shown in Table III, $\log (k_1\tau_0)$ is in good agreement with the experimentally determined apparent $pK_{a_1}^*$'s, which follow the sequence of the excited-state lifetimes but not of their basicities. It is obvious that the main condition for obtaining an apparent $pK_{a_1}^*$ from which the real $pK_{a_1}^*$ value can be deduced is that $k_2\tau_0' \gg 1$ so that $pK_{a_1}^* = pK_{a_1}^*(\text{app}) - \log (\tau_0/\tau_0')$; this is of course not the case for our complexes.

6. Quenching by Organic Buffers. During a quenching study of excited $Ru^{2+}(TAP)_3$ by an oxidizing agent such as the persulfate $S_2O_8^{2-}$, we observed a buffer effect on the luminescence. At that time, those quenching experiments were conducted in the presence of an equimolar acetic acid–acetate buffer at pH 4.7 in order to suppress any pH effect. Under these conditions, the Stern–Volmer (SV) plots of I_0/I or τ_0/τ versus the persulfate concentration (Figure 9A) are curved and the luminescence intensity, even with small amounts of $S_2O_8^{2-}$, is abnormally low. This observation, combined with the fact that the SV plot becomes linear in the absence of buffer (Figure 9B), with much higher luminescence intensities, shows that the buffer interferes in some way with the $S_2O_8^{2-}$ quenching process. This conclusion led us to conduct the experiment in the presence of the buffer alone, which shows indeed that the $Ru^{2+}(TAP)_3$ luminescence is quenched at pH 4.7, where no inhibition by protonation is observed. On the other hand, acetate ion is inactive, so that the quenching effect has to be attributed to the acetic acid.

We tried to test the generality of this observation with other buffers; it turned out that not only the acetic buffer but also the citric and tartaric buffers quench the luminescence of $Ru^{2+}(TAP)_3$ and of the two mixed-ligand complexes; a phosphate buffer, however, has no effect.

In Figure 10, we plotted τ/τ_0 for $Ru^{2+}(TAP)_3$ versus the logarithm of the acid concentration in equimolar acid–base buffers. It can be seen that the quenching appears at lower acid concentrations when the pH of the buffer decreases, and it depends also on the nature of the acid at the same pH (for instance acetic and citric acid at pH 4.7).

The plots of I_0/I and τ_0/τ versus the equimolar concentration of the acid and the conjugated base give the same curve (Figure 11a). The curvature is also observed with the citric buffer at

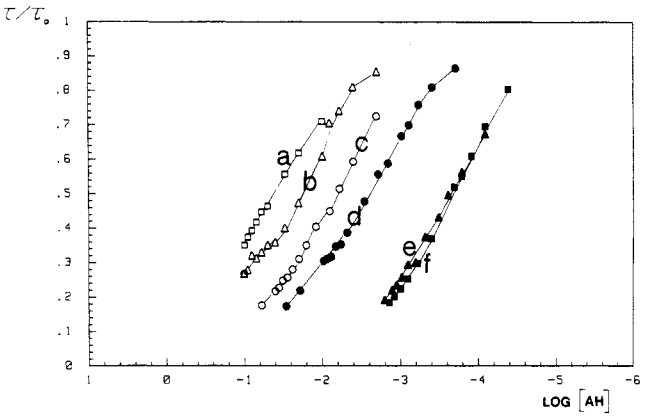

Figure 10. τ/τ_0 for $Ru^{2+}(TAP)_3$ versus the logarithm of the acid concentration in equimolar acid–base buffers: (a) citric buffer at pH 6.4; (b) acetic buffer at pH 4.7; (c) tartaric buffer at pH 4.4; (d) citric buffer at pH 4.7; (e) tartaric buffer at pH 3; (f) citric buffer at pH 3.1.

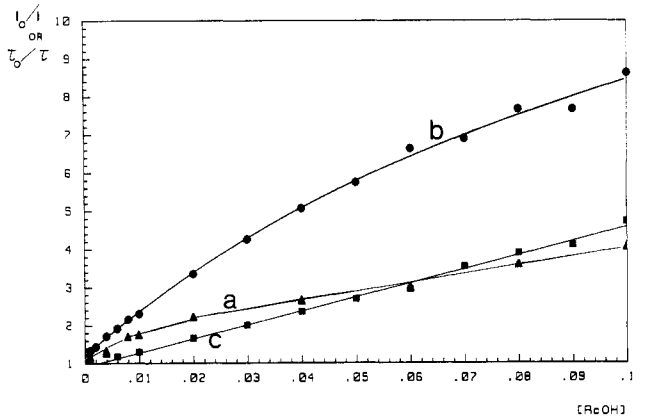

Figure 11. Stern–Volmer plots for 5×10^{-5} M $Ru^{2+}(TAP)_3$: (a) I_0/I and τ_0/τ as a function of the equimolar concentration of acetic acid and acetate at constant pH = 4.7; (b) I_0/I as in (a), but with 0.1 M LiCl; (c) I_0/I as a function of the acetic acid concentration, with a constant acetate concentration of 0.1 M, pH ≥ 4.7.

Table IV. Quenching Rate Constants (k_q) Determined from the Linear SV Plots I_0/I versus the Acid Concentration in the Presence of a Constant Concentration (0.1 M) of the Conjugated Base

complex	buffer	pH	k_q, M^{-1} s^{-1}
$Ru^{2+}(TAP)_3$	acetic	>4.7	1.7×10^8
	citric	>6.4	9×10^7
$Ru^{2+}(TAP)_2(bpy)$	acetic[a]	(4.7)	(3.7×10^8)
	acetic	>4.7	3.6×10^8
	citric	>6.4	2.5×10^8
$Ru^{2+}(TAP)(bpy)_2$	acetic[a]	(4.7)	(5.4×10^8)
	acetic	>4.7	4.7×10^8
	citric	>6.4	3.1×10^8

[a] The values in parentheses are obtained from plots of τ_0/τ versus the equimolar acid–base concentration; under these conditions straight lines are obtained with the mixed-ligand complexes and the acetic buffer.

pH 3.1, 4.7, and 6.4 (corresponding to the three pK_a values of citric acid) and with the tartaric buffer at pH 3.0 and 4.4 (the two pK_a values of tartaric acid); it occurs also with the two mixed-ligand complexes with the citric buffer. In two cases, however, the curvature has not been found: with $Ru^{2+}(bpy)_2(TAP)$ and the $Ru^{2+}(bpy)(TAP)_2$ the SV plots are linear as a function of the equimolar acetic acid–acetate buffer concentration. Their corresponding quenching rate constants are given in Table IV (values in parentheses).

Most of our results concerning the buffer effects are of course very qualitative since (except for the two mixed-ligand complexes with the acetic buffer) the quenching rate constants cannot be determined due to the curvature of the SV plot. Experimental

conditions should thus be found to obtain linear plots.

Curvatures such as those in Figure 11a have already been observed in the literature for the quenching of $Ru^{2+}(bpy)_3{}^*$ by $S_2O_8{}^{2-}$[18] and of several excited Ru(II) polypyridine complexes by heteropolytungstate anions;[19] they have been attributed to the presence of ion pairs between the complex cation and the quenching counterion. If ion pairs were to play any role in our systems, the SV plots should be affected by increased ionic strength. This is indeed the case: as shown in Figure 11b, the addition of 0.1 M LiCl influences the SV plot, which does not become quite linear but the quenching efficiency has increased. If the experiment is performed in the presence of a constant acetate concentration of 0.1 M (Figure 11c), the quenching efficiency becomes lower again but the SV plot is now linear. This effect of such a constant conjugate base concentration is also observed for the citric buffer. Table IV gives the values of the quenching rate constants determined from the linear SV plot so obtained; it is clear that, for the same acid, k_q increases with the basicity of the excited complex and, for the same complex, k_q is slightly smaller with the citric buffer at pH $\geq$ 6.4 than with the acetic buffer at pH $\geq$ 4.7.

7. Discussion of the SV Plots. The first question one should address is of course why the SV plots are curved and why they become linear in the presence of a constant concentration (0.1 M) of the base of the buffer. Since the systems are sensitive to ionic strength, it may be possible that ion pairs would play a certain role in the quenching mechanism by the acid, as in Scheme II, where C stands for the complex, AH for the acid, and B for its conjugated base.

Scheme II

$$C + B \rightleftharpoons C\cdots B \quad K$$

$$C \rightarrow C^* \quad (1-\alpha)I_0$$

$$C^* \xrightarrow{k_d + k_l} C$$

$$C^* + AH \xrightarrow{k_q} C + AH$$

$$C\cdots B \xrightarrow{h\nu} C^*\cdots B \; I_0\alpha$$

$$C^*\cdots B \xrightarrow{k_d + k_l} C\cdots B$$

$$C^*\cdots B + AH \xrightarrow{k_q'} C\cdots B + AH$$

We assume that there is an equilibrium between the free ground-state complex C and its ion pair C···B formed with the conjugated base as counterion; C or C···B may absorb light with the same absorption coefficient (there is no influence of the nature or of the concentration of the counterion in the absorption spectrum), and C* or C*···B can decay to the ground state with the same radiative (k_l) and nonradiative (k_d) deactivation rate constant (no influence of the counterion on the luminescence lifetime and spectra has been detected). The key assumption to explain the curvature of the SV plot is to assume that the acid quenches C* and C*···B with different rate constants, k_q and k_q', respectively. This can be rationalized by considering that the quenching is due to the formation of hydrogen bonds between the carboxylic acid and the free nitrogens of the excited complex; it may then be possible that the presence of the conjugated base in the ion pair would decrease the quenching efficiency because of its tendency to also form hydrogen bonds with the acid; in other words, B would exert some protecting effect of C* against the quenching acid. Assuming a steady-state concentration of the intermediates in Scheme II, one obtains

$$I_0/I = [\tau_0(\tau_0^{-1} + k_q[AH])(\tau_0^{-1} + k_q'[AH])][(1-\alpha) \times (\tau_0^{-1} + k_q'[AH]) + \alpha(\tau_0^{-1} + k_q[AH])] \quad (5)$$

where $\tau_0 = 1/(k_d + k_l)$. If $\alpha = 0$, thus in the absence of ion pairs, eq 5 is linear versus [AH] with a slope equal to $k_q\tau_0$, whereas if $\alpha = 1$, thus when the equilibrium is completely shifted toward the ion pairs, the slope becomes equal to $k_q'\tau_0$. This situation is reached when the SV plots are performed in the presence of a constant and high concentration of the base in the buffer; in contrast, with variable buffer concentrations equimolar in acid and base, a curvature is observed, indicating that for increasing buffer concentrations the quenching becomes less efficient and thus, if Scheme II is correct, that k_q' should be smaller than k_q. In Scheme II, we have not explicitly taken into account an equilibrium in the excited state between the free complex and the ion pair because we assume that the equilibrium for ion pairing is essentially dominated by electrostatic attractions and thus independent of the electronic state of the partners; should, however, the equilibrium in the excited state be shifted relative to its ground-state value, the corresponding calculated I_0/I is also linear as a function of [AH] if the ground- and the excited-state equilibrium are completely shifted toward the ion pair, which would correspond to the experimental conditions where [B] is constant and equal to 0.1 M.

In the experiment of Figure 11b, with a constant 0.1 M LiCl concentration, the presence of a slight curvature in the SV plot would indicate that, at higher buffer concentrations, ion pairs with the acetate are still forming, despite the presence of 0.1 M LiCl.

Some results remain unclear, however, such as the linearity of the SV plot with the two mixed-ligand complexes as a function of the equimolar acetic acid–acetate buffer concentration; the quenching rate constant which is obtained in that case is the same as the one obtained with a constant concentration of the base (Table IV). It may be argued either that the equilibrium constant for the ion pair formation is higher in these two cases than for $Ru^{2+}(TAP)_3$ so that the additional acetate has no effect or that $k_q = k_q'$ (eq 5). In favor of this second hypothesis, one could imagine that, the basicity of the excited mixed-ligand complexes being greater than that of $Ru^{2+}(TAP)_3{}^*$, the presence of B in C*···B would no longer be sufficient to cause a slower quenching of C*···B by AH. If this is true, it would mean that the "protection effect" of B against the quenching of C* by AH should be more efficient with the citrate since with an equimolar citric acid–citrate buffer the mixed-ligand complexes give curved SV plots; this is however not very convincing because the difference between the rate constant values with the acetic and citric acid buffers is not very important (Table IV). On the other hand, one should also keep in mind that, with the citric buffer, the quenching mechanism is probably more complicated than in Scheme II; in that case, indeed, the counterion B could also play the role of quencher (AH) since it is a polyacid, which should produce a static quenching.

Conclusions

From the evolution of the absorption spectra of the three TAP complexes as a function of the protonating power of the medium, the pK_a values of their first protonation and of the second protonation of $Ru^{2+}(bpy)_2(TAP)$ have been determined. However, it has not been possible, as performed by Crutchley, Kress, and Lever[5] with $Ru^{2+}(bpz)_3$, to evaluate the pK_a's of the other protonations. As mentioned before, this could be due to the fact that the pK_a values are too close to each other.

It has also been shown that the best method to evaluate pK_{a_1} in the excited state of the TAP complexes is the thermodynamic Förster cycle. The pK_a's so obtained are however very unaccurate, mainly, as mentioned before, because the protonated excited species luminesce too far in the red, where the photomultipliers are not sensitive enough. Despite those problems, the Förster pK_a's present a sequence of basicity that is in good agreement with the fact that the basicity of the $(Ru^{3+}–TAP^{\bullet-})^*$ chromophore increases when the ligands are better σ-donors (bpy). In contrast, since the quenchings by protonation are irreversible, the apparent $pK_a{}^*$ values do not follow the basicities of the excited complexes but their luminescence lifetimes.

(18) White, H. S.; Becker, W. G.; Bard, A. J. *J. Phys. Chem.* **1984**, *88*, 1840–1846.
(19) Ballardini, R.; Gandolfi, M. T.; Balzani, V. *Inorg. Chem.* **1987**, *26*, 862–867.
(20) Rochester, C. H. *Acidity Functions*; Academic: New York, 1970; p 26.

Concerning the quenchings by the organic buffers, it is the first time, to our knowledge, that such effects have been pointed out with the Ru(II) complexes. Since these quenchings occur in a pH domain where quenching by protonation is absent, they are attributed to formation of hydrogen bonds between the acid and the free nitrogen atoms of the excited complex. The associated mechanism is rather complicated because ion pairs participate in the quenching process; therefore, the reaction scheme that we propose is certainly oversimplified. Under the conditions of linear SV plots, the quenching rate constant by the organic acid increases with the basicity of the excited complex and the acidity of the buffer but never reaches the diffusion limit. This quenching seems characteristic of carboxylic acid since a phosphoric acid–phosphate buffer, alcohols, and sugars such as glucose have no effect on the luminescence lifetimes of the TAP complexes.

Acknowledgment. We are grateful to A. Masschelein and Professor E. Vander Donckt for their helpful discussions about this work. L.J. thanks the IRSIA (Institut pour l'Encouragement de la Recherche Scientifique dans l'Industrie et l'Agriculture) for a fellowship.

Registry No. $[Ru^{2+}(TAP)_3](PF_6^-)_2$, 88181-61-7; $[Ru^{2+}(bpy)(TAP)_2](PF_6^-)_2$, 117183-29-6; $[Ru^{2+}(bpy)_2(TAP)](PF_6^-)_2$, 117183-31-0; $[Ru^{2+}(TAP)_3]H^+$, 117183-32-1; $[Ru^{2+}(bpy)(TAP)_2]H^+$, 117183-33-2; $[Ru^{2+}(bpy)_2(TAP)_2]H^+$, 117183-34-3; $[Ru^{2+}(bpy)_2(TAP)_2](H^+)_2$, 117183-35-4; oleum, 8014-95-7; SO_3, 7446-11-9; sodium acetate, 127-09-3; sodium citrate, 68-04-2; citric acid, 77-92-9; sodium hydroxide, 1310-73-2; sulfuric acid, 7664-93-9; acetic acid, 64-19-7; ammonium persulfate, 7727-54-0; tartaric acid, 87-69-4; sodium tartrate, 868-18-8.

Contribution from the Department of Chemistry and Biochemistry and Molecular Biology Institute, University of California, Los Angeles, Los Angeles, California 90024, and Department of Chemistry, University of Florence, Florence, Italy

Characterization of Copper–Nickel and Silver–Nickel Bovine Superoxide Dismutase by ^1H NMR Spectroscopy

Li-June Ming,[†] Lucia Banci,[‡] Claudio Luchinat,[‡] Ivano Bertini,*[,‡] and Joan Selverstone Valentine*[,†]

Received April 7, 1988

Nickel(II) substitution for Zn^{2+} in bovine Cu,Zn-superoxide dismutase has provided information concerning the configurational and spectroscopic properties of Ni^{2+} in the zinc site and also of Cu^{2+} in the copper site (Ming, L.-J.; Valentine, J. S. *J. Am. Chem. Soc.* **1987**, *109*, 4426–4428). The "effective" electronic relaxation time of Cu^{2+} in this derivative is greatly decreased from 2×10^{-9} s in native protein to about 3×10^{-12} s by the magnetic coupling between the paramagnetic Ni^{2+} and Cu^{2+} ions. Consequently, an isotropically shifted ^1H NMR spectrum of this species has been obtained, consisting of resonances from amino acid residues bound to both metal ions. On the basis of azide titration and proton relaxation time measurements on this species, a full assignment of the isotropically shifted signals is presented. The smaller nuclear relaxation rates of the histidyl protons and the smaller differences in the relaxation rates between ortho-like and meta-like protons of the coordinated histidine residues in the copper site in Cu_2Ni_2SOD as compared to those in Cu_2Co_2SOD result from different correlation times and different contributions of relaxation mechanisms in these two derivatives. A reasonable physical picture of proton relaxation in this magnetically coupled system is proposed, and a theoretical fitting is reported. A comparison of the spectra and relaxation rates of this derivative and of M_2Ni_2SOD ($M = Ag^+, Cu^+$) has provided further information on the bridging ligand and on the relaxation mechanisms.

The high-spin Ni^{2+} ion has two unpaired electrons with a spin-triplet ground state. There are low-lying spin-triplet excited states in its four- or five-coordinated complexes, which allow the unpaired electrons to relax rapidly. However, the energy level of the first excited spin triplet is high above that of the ground state in six-coordinated complexes, where the electronic relaxation mechanism is less efficient.[1] As a consequence, the ^1H NMR spectra of nickel complexes with coordination number <6 usually show well-resolved isotropically shifted NMR signals of reasonable narrow line width.[1]

Bovine copper–zinc superoxide dismutase (Cu_2Zn_2SOD)[2] is a dimeric metalloenzyme with two equivalent subunits, each of which binds a Cu^{2+} and a Zn^{2+} ion at a distance of 6.3 Å with the imidazolate ring of the histidine-61 residue serving as a bridging ligand.[3] A scheme of the metal binding site of this protein from X-ray crystallography studies is shown in Figure 1. The native metal ions have been replaced by various other metal ions in different studies.[4] Most recently, Ni^{2+} has been substituted for Zn^{2+} at the zinc site, forming two new metal-substituted derivatives, Cu_2Ni_2SOD and Ag_2Ni_2SOD, and the former was found to have 26–45% of the SOD activity relative to the native enzyme.[5] It was also shown that both derivatives had relatively sharp isotropically shifted ^1H NMR signals. Moreover, the signals of the protons in the copper binding site can be detected and distinguished. We report here a full characterization of these derivatives by means of ^1H NMR spectroscopy and relaxation.

Experimental Section

Bovine Cu_2Zn_2SOD was purchased from DDI Pharmaceuticals, Inc. (Mountain View, CA), as lyophilized powder and was used without further purification. All other chemicals used are commercially available. The two Ni^{2+}-substituted derivatives, Cu_2Ni_2SOD and Ag_2Ni_2SOD, were prepared in 50 mM phosphate buffer at pH 6.5 as previously reported.[5] All the samples for NMR study were concentrated by ultrafiltration using a Centricon microconcentrator with a molecular mass cutoff of 10 000 Da (Amicon Corp., Danvers, MA).

The isotropically shifted ^1H NMR spectra were obtained on an IBM AF200 spectrometer at 200 MHz, a Bruker CXP300 at 300 MHz, and a Bruker CXP90 at 90 MHz. The modified DEFT multipulse sequence was used to suppress water and diamagnetic protein signals.[6] Typical spectra consisted of about 10 000 scans with 8K data points. Chemical shifts were measured from the water signal, which was assumed to be 4.8

[†] University of California, Los Angeles.
[‡] University of Florence.

(1) (a) Bertini, I.; Luchinat, C. *NMR of Paramagnetic Molecules in Biological Systems*; Benjamin/Cummings: Menlo Park, CA, 1986. (b) La Mar, G. N., Horrocks, W. D., Jr., Holm, R. H., Eds. *NMR of Paramagnetic Molecules*; Academic: New York, 1973.
(2) Abbreviations: SOD, superoxide dismutase; $M_2M'_2SOD$, M- and M'-substituted SOD with M in the copper site and M' in the zinc site (the metal ions in the above derivatives have oxidation states of 2+ unless otherwise specified); NMR, nuclear magnetic resonance; FID, free induction decay; NOE, nuclear Overhauser effect; DEFT, driven equilibrium Fourier transform.
(3) Tainer, J. A.; Getzoff, E. D.; Beem, K. M.; Richardson, J. S.; Richardson, D. C. *J. Mol. Biol.* **1982**, *160*, 181–217.
(4) Valentine, J. S.; Pantoliano, M. W. In *Copper Proteins*; Spiro, T. G., Ed.; Wiley: New York, 1981; Chapter 8.
(5) Ming, L.-J.; Valentine, J. S. *J. Am. Chem. Soc.* **1987**, *109*, 4426–4428.
(6) Hochmann, J.; Kellerhals, H. *J. Magn. Reson.* **1980**, *38*, 23–29.

0020-1669/88/1327-4458$01.50/0